Large diversity in nitrogen- and sulfur-containing compatible solute profiles in polar and temperate diatoms.

Dawson, H.M.[1], Heal, K.R.[1], Torstensson, A.[2], Carlson, L.T.[1], Ingalls, A.[1], Young, J.N.[1]

[1]University of Washington, School of Oceanography, Seattle, WA, 98195

[2]Department of Ecology and Genetics, Limnology, Uppsala University, Uppsala, Sweden

Corresponding author J.N. Young, youngjn@uw.edu

Abstract

Intense bottom-ice algal blooms, often dominated by diatoms, are an important source of food for grazers, organic matter for export during sea ice melt, and dissolved organic carbon. Sea-ice diatoms have a number of adaptations, including accumulation of compatible solutes, that allow them to inhabit this highly variable environment characterized by extremes in temperature, salinity and light. In addition to protecting them from extreme conditions, these compounds present a labile, nutrient-rich source of organic matter and include precursors to climate active compounds (e.g. DMS), which are likely regulated with environmental change. Here, intracellular concentrations of 45 metabolites were quantified in three sea-ice diatom species and were compared to two temperate diatom species, with a focus on compatible solutes and free amino acid pools. There was a large diversity of metabolite concentrations between diatoms with no clear pattern identifiable for sea-ice species. Concentrations of some compatible solutes (isethionic acid, homarine) approached 1 M in the sea-ice diatoms, *Fragilariopsis cylindrus* and *Navicula* cf. *perminuta*, but not in the larger sea-ice diatom, *Nitzschia lecointei* or in the temperate diatom species. The differential use of compatible solutes in sea-ice diatoms suggest different adaptive strategies and highlights which small organic compounds may be important in polar biogeochemical cycles.

Introduction

Intense algal blooms within sea ice are often dominated by diatoms and can account for 55 − 65% of Antarctic coastal primary production (McMinn et al. 2010; Torstensson et al. 2015) and can reach densities up to 10 g m^{-3} (Arrigo, 2016). High heterogeneity, difficulties in sampling and paucity of data make modeling sea-ice primary production difficult. However, under-ice and within-ice microalgal blooms likely contribute to the export of organic carbon and other nutrients during seasonal ice melt (Roukaerts et al. 2016; Kim et al. 2019). Ice-algae are also known to be an essential overwintering food source for grazers (Graeve et al. 2018). As ice melts, rapid recycling of ice algal biomass may provide inorganic nutrients that fuel spring phytoplankton blooms.

While measurements of biomass, taxonomy and primary production rates in sea ice exist (van Leeuwe et al. 2018), the influence of the unique physiology of sea-ice algae on polar ecosystems is poorly understood. Sea-ice diatoms have a number of adaptations to survive subzero temperatures, fluctuating salinity and low light (Thomas and Dieckmann, 2003). The strong seasonal cycle requires microalgae to regulate their cellular composition in response to large shifts in their environment (notably temperature, salinity, pH, nutrients, and light) with implications for biogeochemical cycling and ecosystem nutrition (Leu et al. 2010; Torstensson et al. 2019). Adaptations include elevated protein and ribosome concentrations or increased flexibility of enzyme tertiary structure to maintain cellular rates at low temperatures (Toseland et al. 2004; Gianese et al. 2001; DasSarma et al. 2013), elevated concentrations of polyunsaturated fatty acids to increase membrane fluidity, production of ice-binding proteins and exopolymers to alter ice crystal structure and changes in intra- and extra-cellular compatible solute pools (for review see Young and Schmidt, 2020; Deming and Young, 2017).

Compatible solutes

All organisms have compatible solutes within their cells. Compatible solutes are small uncharged compounds that can accumulate to high intracellular concentrations and form hydration shells that stabilize the tertiary structure of proteins and maintain cell metabolism in high salt environments (Anton, 2011). Compatible solutes can be a variety of compounds such as free amino acids and derivatives, quaternary ammonium compounds, tertiary sulfonium compounds, sugars, and sugar alcohols (Slama et al. 2015). These compounds can have a variety of roles in the cell, including cryoprotection, osmoprotection, and mitigation of reactive oxygen species. Well known compatible solutes in polar marine diatoms include dimethylsulfoniopropionate (DMSP, Sheehan & Petrou 2020, Kameyama et al 2020), isethionic acid (Boroujerdi et al. 2012;), glycine betaine, proline, and homarine (Krell et al. 2007; Boroujerdi et al. 2012; Dawson et al. 2020). Intracellular concentrations of these compounds increase (up to 3 − 4 fold) with decreasing temperature and increasing salinity (Krell et al. 2007; Lyon et al. 2016). In addition to in situ biosynthesis, the Antarctic sea-ice diatoms *Nitzschia lecointei*, *Navicula* cf. *perminuta* and *Fragilariopsis cylindrus* can take up glycine betaine from the environment under high salinity (Torstensson et al. 2019). Unlike in bacteria (Firth et al. 2016), *N. lecointei* does not respire this acquired GBT or convert it to larger macromolecules. Instead, any GBT taken up by *N. lecointei* is retained as a small, soluble molecule in the cell, presumably for exclusive use as a compatible solute (Torstensson et al. 2019).

Characterization and quantification of compatible solutes in marine algae, and sea-ice algae in particular, is still understudied. Most research has focused on one or two diatom species and a few known compatible solutes (Boroujerdi et al. 2012, Krell et al. 2007, Lyon et al. 2011,

2016). While some compatible solutes are likely in high abundance in many diatoms, the wide range of compounds that can be utilized as compatible solutes suggests there is large variation among phytoplankton groups and even between diatom species. For example, isethionic acid was shown to be important in *Fragilariopsis cylindrus* (Boroujerdi et al. 2012) though it was not detected in high abundance in the sea-ice diatom, *N. lecointei* (Dawson et al. 2020). Likewise, homarine has been detected in mesophilic diatoms (Heal et al. 2019) and in *Nitzschia*-dominated, bottom sea-ice samples from the Arctic but was not detected in cultures of *N. lecointei* (Dawson et al. 2020). Recently, the compound, 2,3-dihydroxypropane-1-sulfonate (DHPS), was found to be a potential compatible solute in diatoms (Durham et al. 2019) and at high concentrations in *N. lecointei* (Dawson et al. 2020). Many of these compatible solutes contain nitrogen and sulfur, therefore the rapid regulation, uptake and release of these compounds in response to changing temperature and salinity likely have an impact on biogeochemical cycles. Nitrogen-containing compatible solutes could be an important organic source for heterotrophic catabolism, which would provide regenerated nitrogen within the upper water column to support phytoplankton growth. Volatile sulfur compounds originating from compatible solutes (e.g. DMS) can impact climate and may structure interspecies interactions (Bullock et al. 2017). Thus, nitrogen- and sulfur-containing compatible solutes were characterized in a range of sea-ice diatoms, to determine if their profiles significantly differ from more temperate species.

Approach

This study quantifies intracellular concentrations of a range of nitrogen- and sulfur-containing compatible solutes and free amino acids in three sea-ice diatoms (*Nitzschia lectointei, Fragilariopsis cylindrus* and *Navicula* cf. *perminuta)* and two temperate diatom

species (*Thalassiosira pseudonana*, and *Navicula pelliculosa)*. Cultures and metabolomic extractions were leveraged from previous studies (Torstensson et al. 2019; Heal et al. 2019; Heal 2018) and samples were reanalyzed with an entirely new question in mind: does adaptation to the extreme sea-ice environment fundamentally change compatible solute composition in diatoms? This work will help characterize the organic composition of sea-ice diatoms with the aim of better understanding their role in organic matter cycling and ecology in polar ecosystems.

Methods

Culture maintenance/growth conditions

Axenic cultures of three Antarctic sea-ice diatoms (*N. lecointei*, *N.* cf. *perminuta*, and *F. cylindrus*) and two temperate diatoms (*T. pseudonana* and *N. pelliculosa*) were chosen for study. The exact cultures presented here were examined in previous studies as follows: *N. lecointei*, *N.* cf. *perminuta*, and *F. cylindrus* in Torstensson et al. (2019), *T. pseudonana* in Heal et al. (2019), and *N. pelliculosa* in Heal (2018). *N. lecointei* and *N.* cf. *perminuta,* were isolated from Antarctic bottom sea ice in 2011 (Torstensson et al. 2013, Aguirre et al. 2018). *F. cylindrus* strain CCMP1102, *T. pseudonana* CCMP1335 and *N. pelliculosa* CCMP 543 were purchased from NCMA Bigelow.

Antarctic species were grown at -1°C and a PAR irradiance of 45 μmol photons m^{-2} s^{-1} (16:8 light:dark cycle) using cool white lights. Temperate species were grown at 13°C and a PAR irradiance of 120 μmol photons m^{-2} s^{-1} (12:12 light:dark cycle). In both cases, light was saturating. All cultures were grown in 50 mL borosilicate glass tubes with 35 mL of filter sterilized artificial seawater media with f/2 nutrients (Guillard 1975). Cultures were grown in artificial seawater (ESAW, salinity 31, for Antarctic species, Harrison et al. 1980, and Instant

Ocean, salinity ~35 for temperate species). Cobalamin (vitamin B_{12}), replete in all cultures, was included in the Antarctic culture media as per the f/2 recipe but was added separately at 200 pM to the temperate culture media (Heal et al. 2019, Heal 2018). Antarctic species were confirmed to be axenic via DAPI fluorescent staining and temperate cultures were confirmed to be axenic via marine purity test broth (Saito et al., 2002).

For the Antarctic species, growth rate (n = 2) and cell biovolume (Hillebrand et al. 1999) were determined using light microscopy as described in Torstensson et al. (2019). For the temperate species, growth rates were determined for cultures (n = 9) via the increase in relative fluorescence units (RFU) using a Turner fluorometer (Heal et al. 2019, Heal 2018) and confirmed by cell counts for *T. pseudonana* using a Beckman Coulter Z2 Particle Count and Size Analyzer (Beckman Coulter) and light microscopy for *N. pelliculosa* as it is a colonial species (Lund et al., 1958). There was good agreement between RFU and cell counts ($R^2 > 0.9$), so RFU was converted to cell density on filters at day of harvest for the temperate species (Heal et al. 2019, Heal 2018).

To explore the effect of growth conditions on metabolic profiles using non-metric dimensional scaling analysis, samples were included of *N. lecointei* grown at temperatures -1 and 4 °C, and salinities 32 and 41 (Dawson et al. 2020) and *T. pseudonana* grown at under cobalamin and/or light limitation (Heal et al. 2019). Culture maintenance and growth condition details for these cultures are discussed in detail in Dawson et al. (2020) and Heal et al. (2019). Data processing and analysis for these intraspecific variation samples were carried out exactly as detailed below for the present samples.

Metabolite extraction and LC-MS methods

Cells were harvested during exponential growth onto 47 mm 0.2 μm PTFE filters (Omnipore) using combusted glassware and gentle filtration and stored at –80 °C until extraction. For each biological replicate (n = 2 for Antarctic species, n = 3 for temperate species), two 35 mL cultures were harvested onto each filter. An un-inoculated media blank was prepared and treated in the same manner as samples. Cellular metabolites were extracted using a modified Bligh Dyer extraction (Bligh and Dyer 1959) as described in detail in Boysen et al. (2018), which resulted in a non-polar organic fraction and a polar aqueous fraction. In this study, metabolites of interest were in the polar fraction and so only this fraction was analyzed. To aid in normalization, a cocktail of internal standards was added (listed in Tables S1 and S2, depending on sample as listed in Table S3) before and after extraction (Boysen et al. 2018). Metabolites were analyzed by liquid chromatography–mass spectrometry using a Waters Acquity I-Class UPLC fitted with a SeQuant ZIC-pHILIC column. Mass spectrometry data were acquired using a Thermo QExactive HF (QE) with electrospray ionization (ESI) with polarity switching (full method in Boysen et al. 2018). Data were acquired in two separate runs, as noted in Table S3. A pooled sample was injected at full and half strength throughout the run to monitor instrument stability and train downstream normalization. In addition, a mix of standards in water and a representative matrix at known concentrations was injected at the start and end of the run for quantification, as detailed below.

Data processing

Masses of ions corresponding to metabolites (as listed in Table S4) were integrated using Skyline for small molecules (MacLean et al. 2010), and integrated peaks were run through in-house quality control (QC) and best-matched internal standard (B-MIS) normalization as in

Boysen et al. (2018). Full and abbreviated compound names are listed in Table S4. Abbreviated names are used in figures throughout. Leucine and isoleucine did not chromatographically separate well, so were integrated as a combined signal, referred to here as (iso)leucine. For QC, peaks that did not meet minimum criteria set to ensure correct compound identification and peak quality (listed in Table S5) were excluded from further analysis and referred to as "not detected". Glycine is referred to as "not measured" in *T. pseudonana* since glycine has a *m/z* below the *m/z* scan range used in the associated data acquisition run and thus could not be detected or quantified in those samples. For peaks that passed through quality control, a 30 % improvement to the relative standard deviation (RSD) of each compound in a pooled sample was used as the criteria to apply normalization for the sea-ice diatom and *N. pelliculosa* data, using tools in the B-MIS normalization package to determine this value (Boysen et al. 2018). A 20 % improvement threshold was used to apply normalization for *T. pseudonana* data, exactly as in Heal et al. (2019). Any compounds with a raw RSD of < 10% across the raw pooled areas were not normalized, similar to previous work (Heal et al. 2019). For B-MIS normalization, samples were only adjusted within the same run, not between runs.

Metabolite abundances

Intracellular concentrations were calculated from peak areas for the compounds presented here using three approaches. For metabolites where isotopically-labeled standards were added to samples as a part of the internal standard suite (Tables S1 and S2, depending on sample as listed in Table S3) concentrations were calculated directly (labeled "isotopologue" in quantification method of Table S6). For compounds without isotopologues, a compound-specific response factor (RF) and response factor ratio (RF_{ratio}, as in Boysen et al. 2018) were calculated used to

correct for ion suppression using authentic standards mixed into water and a representative matrix (details outlined in supplemental methods of Boysen et al. 2020; Heal 2018 and labeled "direct RF and RFratio" in quantification methods of Table S6). For a final set of compounds for measured before acquiring authentic standards, a RF for the compound was estimated using a proxy standard that had been run in all sample sets that share the same column, ionization, and structural similarity (assuming a consistent relative RF between the proxy compound and analyte). For these later-acquired compounds, RF_{ratio} was calculated from a later run once an authentic standard was acquired in the same manner as above (labeled "relative RT and RFratio" in quantification methods of Table S6). For example, the *T. pseudonana* data were acquired before the standard for trigonelline was acquired; for those samples, an established homarine RF was used (another aromatic betaine) to estimate a RF assuming a similar homarine/trigonelline ratio in RFs. Then, the RF_{ratio} calculated for trigonelline in the later run, which included a trigonelline standard in a comparable matrix, was used for the *T. pseudonana* run. For any compound in which the ambient matrix signal was larger than the signal of the authentic standard in representative matrix, a RF_{ratio} of 1 was assumed rather than using the calculated value (labeled "RFratio assumed" in quantification methods of Table S6). For detailed compound and sample set quantification details, see Table S6.

Intracellular concentrations in culture were expressed in terms of millimolar intracellular concentration, using cell volume as estimated by microscopy following Hillebrand et al. (1999) for Antarctic species (Torstensson et al. 2019) and from literature values for temperate species (Durham et al. 2019), as listed in Table 1. Cell volumes used for the additional experimental growth conditions are exactly as in Heal et al. (2019) and Dawson et al. (2020). DMSP may volatilize during sample processing resulting in some loss of this compound (Spielmeyer and

Pohnert, 2010). Good agreement among replicates suggests that losses are similar across samples and therefore estimated intracellular concentrations can be taken as a minimum value.

Statistical approaches

For multivariate analysis, intracellular concentrations were standardized to the maximum intracellular concentration observed for each compound across all samples. A nonmetric approach was used to accommodate for the high variable to sample ratio and the non-normal distribution of peak areas across samples. A non-metric dimensional scaling (NMDS) analysis (Kruskal and Wish, 1978) was used based on a Euclidean distance matrix of standardized peak areas to visualize overall differences between samples; dimensionality of the NMDS was assessed by examining a scree plot and calculated the probability with a Monte Carlo permutation. Data transformation, standardization and NMDS were performed in R using the vegan (v2.5-6), and MASS (v7.3.51.5) packages in R (v4.0-0).

Results

Growth rates and cell volume of different diatoms

All samples for metabolomic analysis were collected during exponential growth under replete conditions and were previously analyzed for other studies (Torstensson et al 2019; Heal et al. 2019; Heal 2018). Culture growth rates and cell volumes for the sea-ice diatoms are published (Torstensson et al. 2019). Growth rates for the temperate diatoms were published in Heal et al. (2019) and Heal (2018). Cell volumes for temperate species were previously reported in Durham et al. (2019). This information is summarized in Table 1.

All sea-ice diatoms grown at -1 °C had specific growth rates close to 0.2 d^{-1} (Torstensson et al. 2019) whereas the temperate diatoms grown at 13 °C had specific growth rates of ~0.7 d^{-1} and 0.5 d^{-1} for *T. pseudonana* and *N. pelliculosa*, respectively (Heal et al. 2019; Heal 2018). Measured cell volumes for polar diatoms ranged from 22, 75, and 190 μm^3 for *F. cylindrus, N.* cf. *perminuta* and *N. lecointei*, respectively (Torstensson et al. 2019) whereas both temperate diatoms had reported cell volumes in the middle of this range, 60 and 50 μm^3 for *T. pseudonana* and *N. pelliculosa*, respectively (Durham et al. 2019).

Metabolite overview

A total of 45 metabolites could be quantified and are ranked according to their abundance averaged across all species in Figure 1. Many well-known compatible solutes (e.g. homarine, proline, DHPS, glutamic acid, DMSP) are the most abundant though their concentrations vary widely between species. Full quantification data is shown in Table S7.

Stacked intracellular concentrations of 45 quantified metabolites for each diatom species is shown in Figure 2. *F. cylindrus and N.* cf. *perminuta* had considerably higher total measured metabolite pools (~ 4 M and ~ 3 M, respectively) compared to *N. lecointei* (500 mM) and the temperate diatoms. This is predominantly driven by large intracellular pools of 3 − 4 metabolites. In both *F. cylindrus* and *N.* cf. *perminuta*, homarine and glutamic acid are highly abundant. *N.* cf. *perminuta* also has a high concentration of proline, whereas *F. cylindrus* has high concentrations of ornithine and isethionic acid. While at lower concentrations, major metabolites in *N. lecointei* include DMSP and DHPS, in *T. pseudonana* include homarine (along with glutamic acid and proline) and in *N. pelliculosa* include arginine and proline.

Non-metric dimensional scaling (NMDS) based on the proportional concentrations of all measured metabolites was used to explore the relationships between different species (full list of metabolites and concentrations shown in Table S7). To compare interspecific variation in metabolite pools with intraspecific variation under different growth conditions, data from experimental growth conditions of *N. lecointei* (temperatures -1 and 4˚C, and salinities 32 and 41, Dawson et al. 2020) and *T. pseudonana* (cobalamin and/or light limitation, Heal et al. 2019) were also included. While separation within a species due to growth conditions could be observed in non-dimensional space, all species were clearly separated from each other regardless of growth conditions (Figure 3).

Sulfur-containing compatible solutes

Cellular concentrations of select S-containing compatible solutes and metabolites involved in cell-cell interactions are shown in Table 2. DMSP was present in all strains except *N. pelliculosa*. Within the sea-ice diatoms, *F. cylindrus* is noticeable in lacking DHPS but has high concentrations of isethionic acid (~ 1 M) and taurine (~ 340 mM), which are both at sub-millimolar concentrations or below detection in the other diatom species tested (here and Durham et al. 2019). *N.* cf. *perminuta* has high concentrations of DHPS (~ 200 mM) and cysteic acid (~ 40 mM) whereas DHPS is the only sulfonated compatible solute tested that had a high concentration in *N. lecointei* (~ 75 mM).

Nitrogen-containing compatible solutes

Nitrogen-containing metabolites, particularly quaternary amines, are known to be important compatible solutes in sea-ice diatoms, though few studies have quantified intracellular

concentrations. Table 3 shows selected nitrogenous compounds known to function as compatible solutes. *F. cylindrus* is enriched in homarine and ornithine (~ 700 mM). *N.* cf. *perminuta* is enriched in homarine (> 800 mM) and also proline (> 600 mM). Of the selected N-containing metabolites in Table 3, only glycine betaine is of a reasonably high concentration in *N. lecointei.* Interestingly, glycine betaine is a widely used compatible solute and has a similar concentration (~ 20 mM) across all species with the exception of *N. pelliculosa*, where it was not detected. Other possible nitrogenous compatible solutes, such as ectoine (Fenizia et al. 2020) and proline betaine (Bashir et al. 2014), were not found in high concentrations.

Free amino acid pools

A selection of free proteinogenic amino acids was quantified (concentrations in Supplementary Table S7). *N.* cf. *perminuta* and *F. cylindrus* (pools totaling ~ 1.5 M and ~ 1 M, respectively) had higher free amino acids compared to the other species (< 400 mM) (Figure 4). Besides proline, glutamic acid is a major pool and to a lesser extent alanine, arginine and aspartic acid. In addition, lysine and tyrosine were also significant pools in *F. cylindrus*.

Discussion

Diversity in compatible solute profiles is indicative of multiple functions and complementary pathways

Isethionic acid was the most abundant metabolite measured, ~1M in *F. cylindrus,* though < 1 mM in the other two sea-ice diatoms and not detected in either temperate species. Its precursor, taurine, is also highly abundant (340 mM) in *F. cylindrus* compared to the other diatoms (< 1 mM). A survey of marine phytoplankton and bacterial cultures by Durham et al.

(2019) found isethionic acid in temperate diatoms, *Pseudo-nitzschia pungens* (20 mM) and *Cyclotella meneghiniani* (4 mM), though not in any of the other cultures. The prevalence of *F. cylindrus* in both sea ice and pelagic polar environments, coupled with high concentrations of isethionic acid found within *F. cylindrus* cultures (this study and qualitatively in Boroujerdi et al. 2012) and environmental sea-ice samples (Dawson et al. 2020), suggest that isethionic acid may be potentially important in polar biogeochemical cycles.

In contrast to isethionic acid, another sulfonate, DHPS, was not detected in *F. cylindrus,* despite being widespread in other diatoms and coccolithophores, (this study and Durham et al. 2019), and within seawater and sea ice (Durham et al. 2015; Dawson et al. 2020; Boysen et al. 2020). While intracellular concentrations of DHPS in *N. lecointei* and *N. pelliculosa* matched those published in Dawson et al. (2020) and Durham et al. (2019), respectively, concentrations in *T. pseudonana* were about 10-fold higher than measured by Durham et al. (2019), possibly due to differing culture conditions. In addition to their roles as compatible solutes, isethionic acid, taurine and DHPS (and DMSP) are involved in algal-bacterial interactions (Durham et al. 2015, Amin et al. 2015, Landa et al. 2019, Mayer et al. 2020). It is interesting to speculate that these different sulfonated pathways fulfill complementary roles in cell homeostasis and cryptic sulfur cycling.

Of the nitrogen-containing compatible solutes we measured, homarine was high in both *F. cylindrus* and *N.* cf. *perminuta,* as was ornithine in *F. cylindrus*. The dinoflagellate *Amphidinium carterae* and haptophyte *Emiliania huxleyi* had 0.2, 0.5 mM homarine, respectively (Keller et al 1999), though another study by Gebser et al (2013) found 20 mM in *E. huxleyi* increasing to 47 mM with a doubling of salinity. Homarine is prevalent in the marine environment, including sea-ice communities (Dawson et al. 2020) and tropical surface waters

(Boysen et al. 2020, Keller et al. 2004), and could potentially be an important organic substrate in marine biogeochemical cycles.

Ornithine is known to act as a compatible solute in higher plants (Slama et al. 2015) but is mostly associated with salt stress in the sea-ice diatom *F. cylindrus* as an alternative precursor to glutamate for proline synthesis (Krell et al. 2007). In diatoms, ornithine is also an important component of the ornithine-urea cycle, which can be used for recycling nitrogen within the cell (Allen et al. 2011). In addition, diatoms use ornithine and its decarboxylated product to anchor polyamines that provide the organic scaffolding for silica frustule synthesis (Kröger et al. 2007). The high concentrations of ornithine in *F. cylindrus* suggest that it is used directly as a major compatible solute though questions remain whether this high concentration also impacts proline synthesis, urea cycling or frustule biosynthesis.

Proline was highly abundant in *N.* cf. *perminuta* (>600 mM). Both Dawson et al. (2020) and Krell et al. (2007) found over 4-fold variation in proline concentrations in response to salinity in *N. lecointei* and *F. cylindrus*, respectively. In contrast, glycine betaine, a well-known compatible solute across many different organisms, has moderate and similar intracellular concentrations across all species tested (except *N. pelliculosa* in which it was absent). Dawson et al. (2020) found no clear pattern of regulation in response to temperature and salinity in *N. lecointei*. Glycine betaine also modulates methylation of gene promoters to regulate gene expression (Figuerosa et al. 2018), and at vacuolar concentrations over 0.1M can enhance diatom buoyancy (Boyd et al. 2002). Glycine betaine abundance is strongly regulated in response to cobalamin availability in *T. pseudonana* (Heal et al. 2019) and between exponential and stationary growth in other eukaryotic algae (Keller et al. 1999). While glycine betaine is an effective compatible solute in sea-ice diatoms via uptake, retention, and release, as shown for *N.*

lecointei in Torstensson et al. (2019), its de novo synthesis may not be strongly regulated by temperature and salinity in sea-ice diatoms.

Free amino acid pools

The free amino acid pool can be utilized for protein synthesis, as stores of metabolic intermediates and as compatible solutes in their own right (Clark et al. 1972). In *N.* cf. *perminuta* and *F. cylindrus* elevated levels of free amino acid pools of alanine, arginine, glutamic acid and aspartic acid were found, which are all elevated in plants under abiotic stress (Mansour et al. 2000). Glutamic acid was particularly large in these species; it is known to act as a compatible solute and is a precursor for proline synthesis (Fujii et al. 1995). High tyrosine in *F. cylindrus* compared to other species (33 mM compared to ≤ 1 mM in others) could be related to the role of tyrosine kinases in regulating cell volume during salt stress (Pasantes-Morales et al. 2006).

Environment and cell size likely factor into the requirement of high intracellular concentrations of compatible solutes.

The large variability in intracellular metabolite concentrations across different diatom species suggests no preference of particular compatible solutes by sea-ice diatoms. Perhaps the general flexibility of diatom metabolism overrides any sea-ice specific response. Alternatively, the similar salinities in our cultures may have masked any sea-ice response, which may only be identifiable under salt stress. Nonetheless, N- and S-containing compatible solute concentrations approaching 1 M in the sea-ice diatoms *F. cylindrus* and *N.* cf. *perminuta* are among the highest concentrations measured in eukaryotic algae although there are few data available. DMSP can reach ~ 1 M in some dinoflagellates and prymnesiophytes (McParland and Levine, 2019) and

glycine betaine can reach close to 1M in halophilic bacteria (Imhoff and Rodriguez-Valera, 1984). Adaptation to a permanently cold, fluctuating salinity environment may have resulted in these two species maintaining high intracellular concentrations of compatible solutes compared to temperate diatoms.

High concentrations of some potential compatible solutes and free amino acids in *F. cylindrus* and *N.* cf. *perminuta* contrasted with the third sea-ice diatom analyzed, *N. lecointei*, that had no uniquely high concentrations of any measured compatible solutes. This could be due to a number of factors, *N. lecointei* may use compatible solutes that we were unable to quantify, may have different intracellular concentrations/pumping of cations (K^+/Na^+) or employ other strategies (e.g. EPS, Steele et al. 2014). *N. lecointei* is considerably larger (190 μm^3) compared to *F. cylindrus* (22 μm^3). An overestimation of cell cytosol volume (e.g. to the presence of large vacuoles) would result in calculated lower intracellular concentrations, though this is unlikely as there is not a consistent trend across all metabolites. The smaller surface area:volume in *N. lecointei* may reduce the need for large intracellular pools of compatible solutes although more species and more conditions are needed before any conclusions can be drawn. Cell size and intracellular concentrations of metabolites are not fixed, and can vary in response to environmental stress. Gebser et al. (2013) found that the haptophye, *E. huxleyi*, will change cell size but maintain compatible solute ratios in response to salinity shifts whereas the dinoflagellate *Prorocentrum minimum* changes compatible solute ratios while maintaining volume. Both Krell et al. (2007) and Dawson et al. (2020) found a $3-4$ fold increase in proline concentrations in response to an upshift in salinity of 36 for *F. cylindrus* and 10 for *N. lecointei*, respectively. Dawson et al. (2020) also found an increase in a number of other compatible solutes, responding to both temperature and salinity, in conjunction with a small change in cell size. This study

provides one of the first surveys of baseline intracellular concentrations of a variety of compatible solutes and amino acids in sea-ice diatoms under nutrient replete, exponential growth, highlighting the diversity in composition. Further research is needed to determine how these profiles may be regulated under varying environmental conditions, as has been shown for other marine environments (Boysen et al. 2020).

Environmental implications

Little is known about the intentional release of compatible solutes during normal growth or rates of cell lysis, but some compatible solutes can be rapidly ejected from the cell in response to a hypoosmotic shock (Torstensson et al. 2019) producing dissolved organic carbon. Dawson et al. (2020) used 'back-of-the-envelope' calculations based on *N. lecointei* and field samples to demonstrate that a large release of the nitrogenous compatible solutes due to ice melt could be a significant source of labile dissolved organic nitrogen. Considering that *N. lecointei* had some of the lowest compatible solute concentrations that were measured here, regulation and release of compatible solutes by sea-ice algae (and the community composition) could be an important missing component of the nitrogen cycling budget in polar oceans.

Author contributions

HD and JY designed the experiment; HD, KH and LC collected data and analyzed results. AT and KH carried out the original culture work and sample collection (as published elsewhere). HD, KH, LC, AT, IA and JY all contributed to the writing of the manuscript.

Acknowledgements

We would like to thank Natalie Kellog, Regina Lionheart and Alec Meyers for assistance in the culturing, microscopic counts and extraction of *T. pseudonana* and *N. pelliculosa* cultures and Alec Meyers for LC-MS run set up. Thanks also to the National Science Foundation (OPP 1925160 to Jim McClintock); the Society of Integrative and Comparative Biology, including its divisions of Comparative Physiology and Biochemistry, Ecology and Evolution, and Invertebrate Zoology; the American Microscopical Society; and The Crustacean Society for support of the Antarctic Symposium. We appreciate the helpful comments of two anonymous reviewers.

Funding

This work was supported by grants from the National Science Foundation (OPP 1744645, JNY) and the Simons Foundation (561645 to JNY; 385428 to AEI; 598819 to KRH).

Data availability statement

The data underlying this article are available in the article and in its online supplementary material, and available in Metabolomics Workbench [unique website link for this study will be added for publication].

References

Aguirre LE, Ouyang L, Elfwing A, Hedblom M, Wulff A, Inganäs O. 2018. Diatom frustules protect DNA from ultraviolet light. Sci Rep 8:5138.

Allen AE, Dupont CL, Oborník M, Horák A, Nunes-Nesi A, McCrow JP, Zheng H, Johnson DA, Hu H, Fernie AR, Bowler C. 2011. Evolution and metabolic significance of the urea cycle in photosynthetic diatoms. Nature 473:203–7.

Amin SA, Hmelo LR, van Tol HM, Durham BP, Carlson LT, Heal KR, Morales RL, Berthiaume CT, Parker MS, Djunaedi B, Ingalls AE, Parsek MR, Moran MA, Armbrust E V. 2015. Interaction and signalling between a cosmopolitan phytoplankton and associated bacteria. Nature 522:98–101.

Antón J. (2011) Compatible Solute. In: Gargaud M. et al. (eds) Encyclopedia of Astrobiology. Springer, Berlin, Heidelberg. https://doi.org/10.1007/978-3-642-11274-4_336

Arrigo KR. 2016. Sea ice as a habitat for primary producers. In: Thomas, D.N. (ed) Sea Ice. Third Ed John Wiley and Sons Ltd, p352–69.doi:10.1002/9781118778371.ch14

Bashir A, Hoffmann T, Kempf B, Xie X, Smits SHJ, Bremer E. 2014. Plant-derived compatible solutes proline betaine and betonicine confer enhanced osmotic and temperature stress tolerance to *Bacillus subtilis.* Microbiol (United Kingdom) 160:2283–94.

Bligh EG, Dyer WJ. 1959. A rapid method of total lipid extraction and purification. Can J Biochem Physiol 37:911–17.

Boroujerdi AFB, Lee PA, DiTullio GR, Janech MG, Vied SB, Bearden DW. 2012. Identification of isethionic acid and other small molecule metabolites of *Fragilariopsis cylindrus* with nuclear magnetic resonance. Anal Bioanal Chem 404:777–84.

Boyd CM, Gradmann D. 2002. Impact of osmolytes of marine phytoplankton. Mar Biol 141:605–18.

Boysen AK, Carlson LT, Durham BP, Groussman RD, Aylward FO, Ribalet F, Heal KR, DeLong EF, Armbrust EV, Ingalls AE. 2020. Diel Oscillations of Particulate Metabolites Reflect Synchronized Microbial Activity in the North Pacific Subtropical Gyre. bioRxiv 2020.05.09.086173.

Boysen AK, Heal KR, Carlson LT, Ingalls AE. 2018. Best-Matched Internal Standard Normalization in Liquid Chromatography–Mass Spectrometry Metabolomics Applied to Environmental Samples. Anal Chem 90:1363–69.

Bullock HA, Luo H, Whitman WB. 2017. Evolution of Dimethylsulfoniopropionate Metabolism in Marine Phytoplankton and Bacteria. Front Microbiol 8: 637 .

Clark VL, Peterson DE, Bernlohr RW. 1972. Changes in free amino acid production and intracellular amino acid pools of *Bacillus licheniformis* as a function of culture age and growth media. J Bacteriol 112:715–25.

Dawson HM, Heal KR, Boysen AK, Carlson LT, Ingalls AE, Young JN. 2020. Potential of temperature- and salinity-driven shifts in diatom compatible solute concentrations to impact biogeochemical cycling within sea ice. Elem Sci Anth, 8(1), p.25. DOI: http://doi.org/10.1525/elementa.421.

Deming JW, Young JN. 2017. The role of exopolysaccharides in cold-adaptation. In: Margesin R, editor. Psychrophiles: from Biodiversity to Biotechnology 2nd Edition, Berlin Heidelberg: Srpinger-Verlag. p. 259–84.

Durham BP, Boysen AK, Carlson LT, Groussman RD, Heal KR, Cain KR, Morales RL, Coesel SN, Morris RM, Ingalls AE, Armbrust EV. 2019. Sulfonate-based networks between

eukaryotic phytoplankton and heterotrophic bacteria in the surface ocean. Nat Microbiol.4: 1706–1715
Durham BP, Sharma S, Luo H, Smith CB, Amin SA, Bender SJ, Dearth SP, Van Mooy BAS, Campagna SR, Kujawinski EB, Armbrust EV, Moran MA. 2015. Cryptic carbon and sulfur cycling between surface ocean plankton. Proc Natl Acad Sci 112:453–57.
Fenizia S, Thume K, Wirgenings M, Pohnert G. 2020. Ectoine from Bacterial and Algal Origin Is a Compatible Solute in Microalgae. Mar Drugs 18:42.
Figueroa-Soto CG, Valenzuela-Soto EM. 2018. Glycine betaine rather than acting only as an osmolyte also plays a role as regulator in cellular metabolism. Biochimie 147:89–97.
Firth E, Carpenter SD, Sørensen HL, Collins RE, Deming JW. 2016. Bacterial use of choline to tolerate salinity shifts in sea-ice brines. Elem Sci Anthr 4:000120.
Fujii S, Nishimoto N, Notoya A, Hellebust JA. 1995. Growth and osmoregulation of *Chaetoceros muelleri* in relation to salinity. Plant Cell Physiol 36:759–64.
Gebser B, Pohnert G. 2013. Synchronized regulation of different zwitterionic metabolites in the osmoadaption of phytoplankton. Mar Drugs 11:2168–82.
Graeve M, Kohlbach D, Vortkamp M, van Franeker JA, Brandt A, Flores H, Schaafsma FL, Lange BA, David C. 2018. Dependency of Antarctic zooplankton species on ice algae-produced carbon suggests a sea ice-driven pelagic ecosystem during winter. Glob Chang Biol 24:4667–81.
Guillard RRL. 1975. Culture of phytoplankton for feeding marine invertebrates. In: Smith WL, Chanley MH, editors. Culture of Marine Invertebrate Animals Boston, MA: Springer.
Heal KR, Ingalls AE. 2018. The power and promise of direct measurements of metabolites in marine systems Seattle]: Thesis (Ph. D.)--University of Washington.
Heal KR, Kellogg NA, Carlson LT, Lionheart RM, Ingalls AE. 2019. Metabolic consequences of cobalamin scarcity in the diatom *Thalassiosira pseudonana* as revealed through metabolomics. Protist 170:328–48.
Hillebrand H, Dürselen C-D, Kirschtel D, Pollingher U, Zohary T. 1999. Biovolume calculation for pelagic and benthic microalgae. J Phycol 35:403–24.
Imhoff JF, Rodriguez-Valera F. 1984. Betaine is the main compatible solute of halophilic eubacteria. J Bacteriol 160:478–79.
Kalamaki MS, Merkouropoulos G, Kanellis AK. 2009. Can ornithine accumulation modulate abiotic stress tolerance in Arabidopsis? Plant Signal Behav 4:1099–1101.
Kameyama, S., Otomaru, M., McMinn, A. and Suzuki, K. (2020), Ice Melting Can Change DMSP Production and Photosynthetic Activity of the Haptophyte Phaeocystis antarctica 1. J. Phycol., 56: 761-774. doi:10.1111/jpy.12985
Keller MD, Kiene RP, Matrai PA, Bellows WK. 1999. Production of glycine betaine and dimethylsulfoniopropionate in marine phytoplankton. II. N-limited chemostat cultures. Mar Biol 135:249–57.
Keller MD, Matrai PA, Kiene RP, Bellows WK. 2004. Responses of coastal phytoplankton populations to nitrogen additions: dynamics of cell-associated dimethylsulfoniopropionate (DMSP), glycine betaine (GBT), and homarine. Can J Fish Aquat Sci 61:685–99.
Kim M, Yang EJ, Kim D, Jeong J-H, Kim HJ, Park J, Jung J, Ducklow HW, Lee S, Hwang J. 2019. Sinking particle flux and composition at three sites of different annual sea ice cover in the Amundsen Sea, Antarctica. J Mar Syst 192:42–50.
Krell A, Funck D, Plettner I, John U, Dieckmann G. 2007. Regulation of proline metabolism under salt stress in the psychrophilic diatom Fragilariopsis cylindrus (Bacillariophyceae). J

Phycol 43:753–62.
Kröger N, Deutzmann R, Bergsdorf C, Sumper M. 2000. Species-specific polyamines from diatoms control silica morphology. Proc Natl Acad Sci U S A 97:14133–38.
Kruskal JB, Wish M. 1978. Multidimensional Scaling. In: Uslaner E, editor. Paper series on Quantitative Applications in the Social Sciences. Vol 07-011. ed Beverly Hills and London: Sage Publications. p. 7–28.
Landa M, Burns AS, Durham BP, Esson K, Nowinski B, Sharma S, Vorobev A, Nielsen T, Kiene RP, Moran MA. 2019. Sulfur metabolites that facilitate oceanic phytoplankton–bacteria carbon flux. ISME J 13:2536–50.
Leu E, Mundy CJ, Assmy P, Campbell K, Gabrielsen TM, Gosselin M, Juul-Pedersen T, Gradinger R. 2015. Arctic spring awakening – Steering principles behind the phenology of vernal ice algal blooms. Prog Oceanogr 139:151–70.
Lund JWG, Kipling C, Le Cren ED. 1958. The inverted microscope method of estimating algal numbers and the statistical basis of estimations by counting. Hydrobiologia 11:143–70.
Lyon BR, Bennett-Mintz JM, Lee PA, Janech MG, Ditullio GR. 2016. Role of dimethylsulfoniopropionate as an osmoprotectant following gradual salinity shifts in the sea-ice diatom *Fragilariopsis cylindrus*. Environ Chem 13:181–94.
MacLean B, Tomazela DM, Shulman N, Chambers M, Finney GL, Frewen B, Kern R, Tabb DL, Liebler DC, MacCoss MJ. 2010. Skyline: an open source document editor for creating and analyzing targeted proteomics experiments. Bioinformatics 26:966–68.
Mansour MMF. 2000. Nitrogen Containing Compounds and Adaptation of Plants to Salinity Stress. Biol Plant 43:491–500.
Mayer J, Huhn T, Habeck M, Denger K, Hollemeyer K, Cook AM. 2010. 2,3-Dihydroxypropane-1-sulfonate degraded by *Cupriavidus pinatubonensis* JMP134: purification of dihydroxypropanesulfonate 3-dehydrogenase. Microbiology 156:1556–64.
McMinn A, Martin A, Ryan K. 2010. Phytoplankton and sea ice algal biomass and physiology during the transition between winter and spring (McMurdo Sound, Antarctica). Polar Biol 33:1547–56.
McParland EL, Levine NM. 2019. The role of differential DMSP production and community composition in predicting variability of global surface DMSP concentrations. Limnol Oceanogr 64:757–73.
Metpally RPR, Reddy BVB. 2009. Comparative proteome analysis of psychrophilic versus mesophilic bacterial species: Insights into the molecular basis of cold adaptation of proteins. BMC Genomics 10:11.
Pasantes-Morales H, Lezama RA, Ramos-Mandujano G. 2006. Tyrosine kinases and osmolyte fluxes during hyposmotic swelling. Acta Physiol 187:93–102.
Roukaerts A, Cavagna A-J, Fripiat F, Lannuzel D, Meiners KM, Dehairs F. 2016. Sea-ice algal primary production and nitrogen uptake rates off East Antarctica. Deep Sea Res Part II Top Stud Oceanogr 131:140–49.
Saito MA, Moffett JW, Chisholm SW, Waterbury JB. 2002. Cobalt limitation and uptake in Prochlorococcus. Limnol Oceanogr 47:1629–36.
Scholz B, Liebezeit G. 2012. Compatible solutes in three marine intertidal microphytobenthic Wadden Sea diatoms exposed to different salinities. Eur J Phycol 47:393–407.
Sheehan, C.E., Petrou, K. Dimethylated sulfur production in batch cultures of Southern Ocean phytoplankton. Biogeochemistry 147, 53–69 (2020). doi.org/10.1007/s10533-019-00628-8
Slama I, Abdelly C, Bouchereau A, Flowers T, Savouré A. 2015. Diversity, distribution and roles

of osmoprotective compounds accumulated in halophytes under abiotic stress. Ann Bot 115:433–47.
Spielmeyer A, Pohnert G. 2010. Direct quantification of dimethylsulfoniopropionate (DMSP) with hydrophilic interaction liquid chromatography/mass spectrometry. J Chromatogr B, Anal Technol Biomed life Sci 878:3238–42.
Steele DJ, Franklin DJ, Underwood GJC. 2014. Protection of cells from salinity stress by extracellular polymeric substances in diatom biofilms. Biofouling 30:987–98.
Thomas DN, Dieckmann G. 2003. Sea Ice: An Introduction to its Physics, Chemistry, Biology and Geology Blackwell Science Ltd.
Torstensson, A., Dinasquet, J., Chierici, M., Fransson, A., Riemann, L. and Wulff, A. 2015, Physicochemical control of sea ice microbial communities. Environ Microbiol, 17: 3869-3881.
Torstensson A, Hedblom M, Andersson J, Andersson MX, Wulff A. 2013. Synergism between elevated pCO_2 and temperature on the Antarctic sea ice diatom *Nitzschia lecointei*. Biogeosciences 10:6391-401
Torstensson A, Young JN, Carlson LT, Ingalls AE, Deming JW. 2019. Use of exogenous glycine betaine and its precursor choline as osmoprotectants in Antarctic sea-ice diatoms. J Phycol 675:663–75.o
Toseland A, Daines SJ, Clark JR, Kirkham A, Strauss J, Uhlig C, Lenton TM, Valentin K, Pearson GA, Moulton V, Mock T. 2013. The impact of temperature on marine phytoplankton resource allocation and metabolism. Nat Clim Change 3:979–84.
van Leeuwe MA, Tedesco L, Arrigo KR, Assmy P, Campbell K, Meiners KM, Rintala J-M, Selz V, Thomas DN, Stefels J, Deming JW. 2018. Microalgal community structure and primary production in Arctic and Antarctic sea ice: A synthesis. Elem Sci Anth 6.(1), p.4. DOI: http://doi.org/10.1525/elementa.267
Venables WN, Ripley BD. 2002. Modern Applied Statistics with S. Fourth Edn. P 498 10.1007/978-0-387-21706-2
Young JN, Schmidt K. 2020. It's what's inside that matters: physiological adaptations of high-latitude marine microalgae to environmental change. New Phytol. 227:5 doi:10.1111/nph.16648

Tables

Table 1. Specific growth rate of axenic diatom cultures. Data show mean ± SD (*n* = 2) unless noted.

Diatom species	Growth Temp (℃)	Specific growth rate (μ d^{-1})	Cell Volume (μm^3)
F. cylindrus[a]	-1	0.19 ± 0.001	22
N. lecointei[a]*	-1	0.22 ± 0.005	190
N. cf. *perminuta*[a]	-1	0.22 ± 0.006	75
T. pseudonana[b]*	13	0.66 ± 0.01	60
N. pelliculosa[b]	13	0.47 ± 0.01	50

[a]Antarctic diatom cultures grown for 140h at 31 ppt salinity and -1˚C. Cell volume as measured by microscopy in Torstensson et al. (2019).
[b]Mesophilic diatom cultures grown for 120h and 144h, respectively, at 35 ppt salinity and 13˚C, *n* = 9. Cell volume based on previously reported values of cell dimension and size as reported in Durham et al. (2019).
*Growth rates for this species under additional experimental culture conditions can be found in table S3.

Table 2: Cellular concentrations of select S-containing compatible solutes

Diatom Species	DHPS (mM)	Cysteic acid (mM)	Sulfolactate (μM)	Isethionic acid (mM)	Taurine (mM)	DMSP (+/-)
F. cylindrus[a]	n.d.	0.200 ±0.028	6 ± 2	**973** ± **90**	**342** ± **1**	+
N. lecointei[a]	76 ± 6	2.2 ± 0.5	40 ± 4	0.94 ± 0.9	0.33 ± 0.3	+
N. cf. *perminuta*[a]	**211** ± **9**	**43** ± **6**	6 ± 1	0.26 ± 0.1	n.d.	+
T. pseudonana[b]	78 ± 8	0.005 ± 0.001	3 ± 0.3	n.d.	0.002 ± 0.0001	+
N. pelliculosa[b]	4.4 ± 3	n.d.	n.d.	n.d.	n.d.	-

[a] sea-ice diatoms
[b] temperate diatoms
n.d. not detected

Table 3: Cellular concentrations (mM) of select nitrogenous compatible solutes

Diatom Species	Glycine betaine	Choline	Homarine	Homoserine	Ornithine	Proline
F. cylindrus	37 ± 8	4 ± 1	**735 ± 200**	17 ± 5	**685 ± 108**	126 ± 23
N. lecointei	20 ± 0.2	4 ± 0.5	1.3 ± 0.9	1 ± 0.1	4 ± 1	49 ± 0.9
N. cf. *perminuta*	25 ± 2	49 ± 4	**830 ± 90**	16 ± 3	43 ± 3	**627 ± 170**
T. pseudonana	18 ± 1	15 ± 2	234 ± 20	1.1 ± 0.2	7 ± 2	104 ± 13
N. pelliculosa	n.d.	0.05 ± 0.01	n.d.	n.d.	10 ± 0.6	86 ± 11

Figure Legends

Figure 1. Left panel: Box and whisker plot of intracellular concentrations of quantifiable metabolites averaged across all species and replicates under optimal growth. X-axis is log-scaled. Right panel: Presence/absence of a metabolite across replicates for each species. A value of 0 indicates it was not detected in that species, 1.0 indicates present in all replicates and between 0-1 it was detected in some but not all replicates. Data summarized in table S7.

Figure 2: Intracellular concentrations (mM) of select metabolites across the five diatom species. Average of triplicates for *T. pseudonana* and *N. pelliculosa* and duplicates for the three sea-ice diatoms. The most abundant 11 molecules for each organism are shown, with compounds that do not fall into this criterion depicted as a summed amount in gray. Crosses and asterisk denote N- and S-containing metabolites, respectively.

Figure 3: Non-metric multidimensional scaling comparing the metabolite composition of five diatom species. Metabolite concentrations are scaled to the total measured metabolite pool for each replicate. Colors match different species and symbols indicate replicates under different growth conditions. Culture information and growth rates for all samples can be found in table S3. Metabolites included and raw intracellular concentrations (mM) for each can be found in table S7.

Figure 4: Stacked bar chart of intracellular concentrations (mM) of quantified free proteinogenic amino acids. Average of triplicates for *T. pseudonana* and *N. pelliculosa* and duplicates for *N. lecointei, F. cylindrus* and *N.* cf. *perminuta.* Concentration data for each species is in table S7.

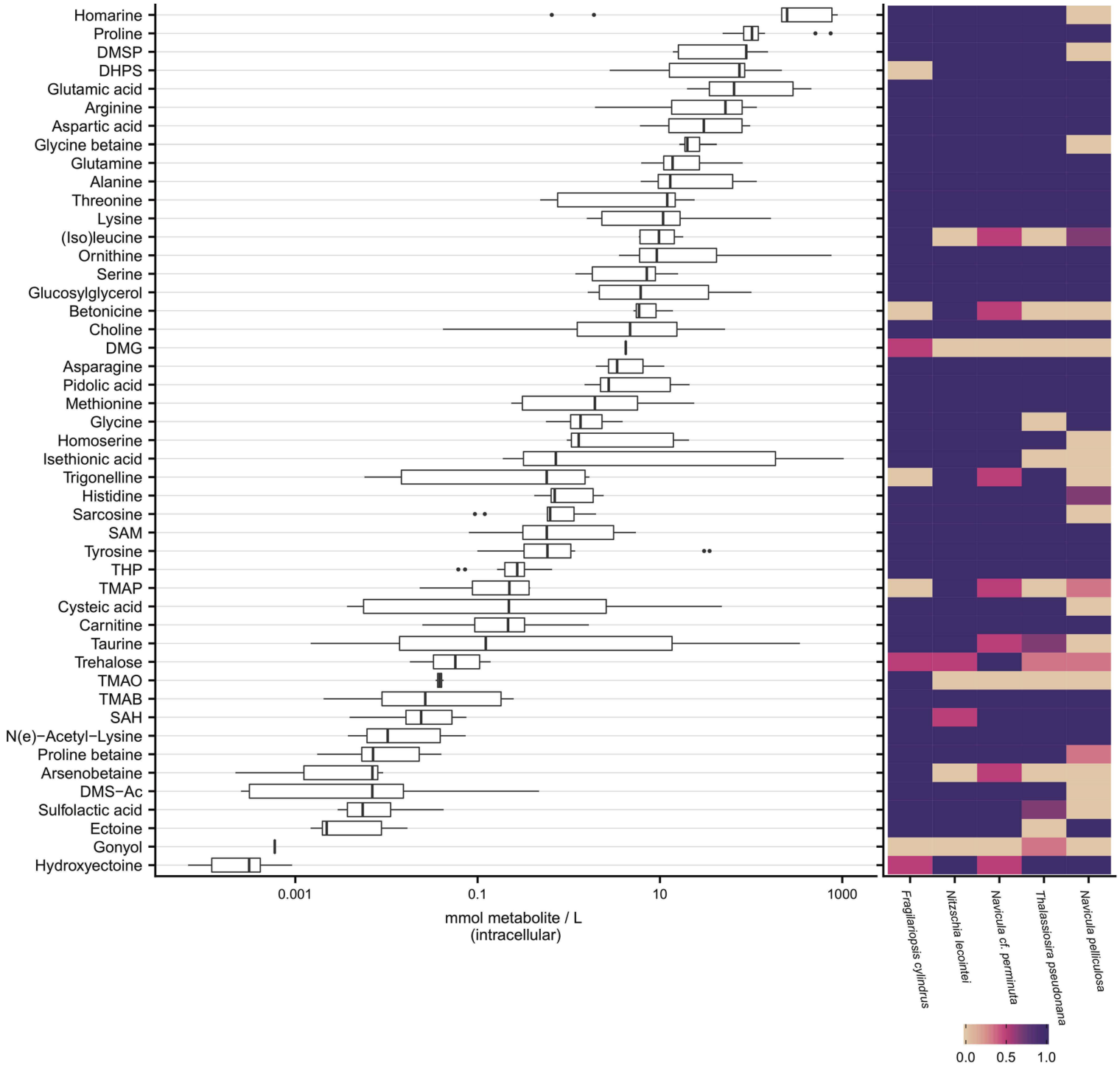
Homarine
Proline
DMSP
DHPS
Glutamic acid
Arginine
Aspartic acid
Glycine betaine
Glutamine
Alanine
Threonine
Lysine
(Iso)leucine
Ornithine
Serine
Glucosylglycerol
Betonicine
Choline
DMG
Asparagine
Pidolic acid
Methionine
Glycine
Homoserine
Isethionic acid
Trigonelline
Histidine
Sarcosine
SAM
Tyrosine
THP
TMAP
Cysteic acid
Carnitine
Taurine
Trehalose
TMAO
TMAB
SAH
N(e)−Acetyl−Lysine
Proline betaine
Arsenobetaine
DMS−Ac
Sulfolactic acid
Ectoine
Gonyol
Hydroxyectoine
0.001
0.1
10
1000
mmol metabolite / L
(intracellular)
Fragilariopsis cylindrus
Nitzschia lecointei
Navicula cf. perminuta
Thalassiosira pseudonana
Navicula pelliculosa
0.0
0.5
1.0

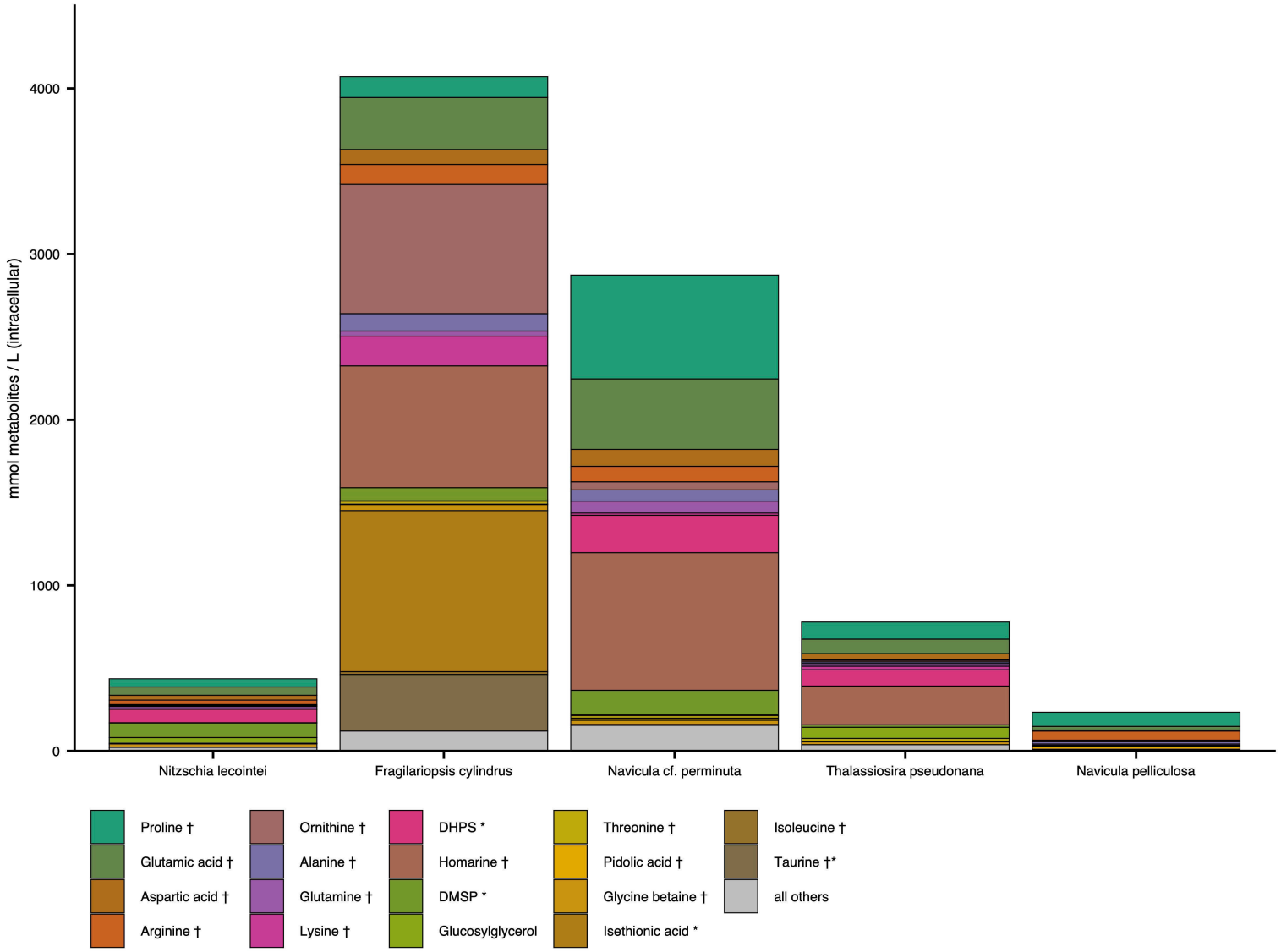
mmol metabolites / L (intracellular)
0
1000
2000
3000
4000
Nitzschia lecointei
Fragilariopsis cylindrus
Navicula cf. perminuta
Thalassiosira pseudonana
Navicula pelliculosa
Proline †
Glutamic acid †
Aspartic acid †
Arginine †
Ornithine †
Alanine †
Glutamine †
Lysine †
DHPS *
Homarine †
DMSP *
Glucosylglycerol
Threonine †
Pidolic acid †
Glycine betaine †
Isethionic acid *
Isoleucine †
Taurine †*
all others

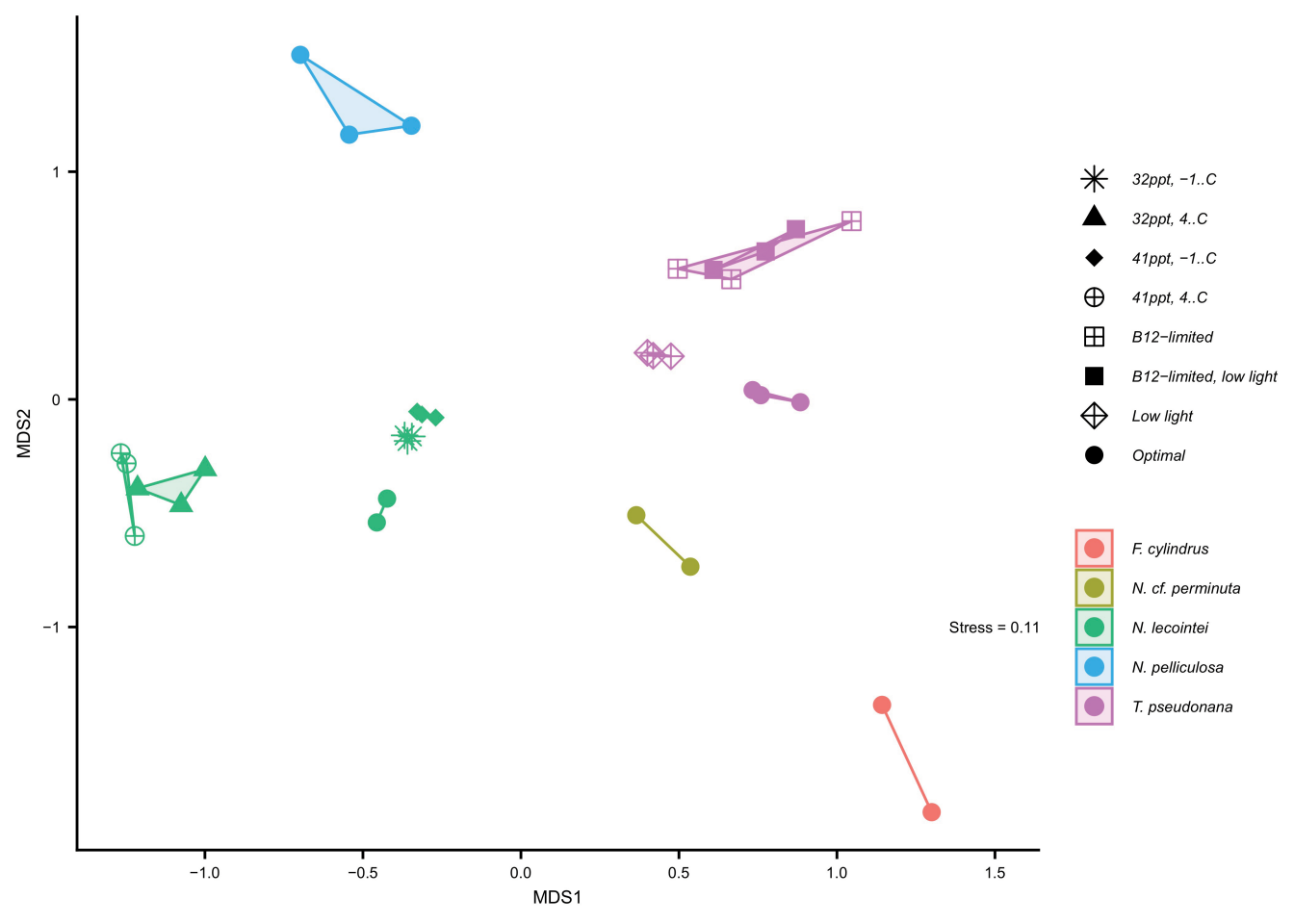
MDS2
MDS1
1
0
−1
−1.0
−0.5
0.0
0.5
1.0
1.5
Stress = 0.11
32ppt, −1..C
32ppt, 4..C
41ppt, −1..C
41ppt, 4..C
B12−limited
B12−limited, low light
Low light
Optimal
F. cylindrus
N. cf. perminuta
N. lecointei
N. pelliculosa
T. pseudonana

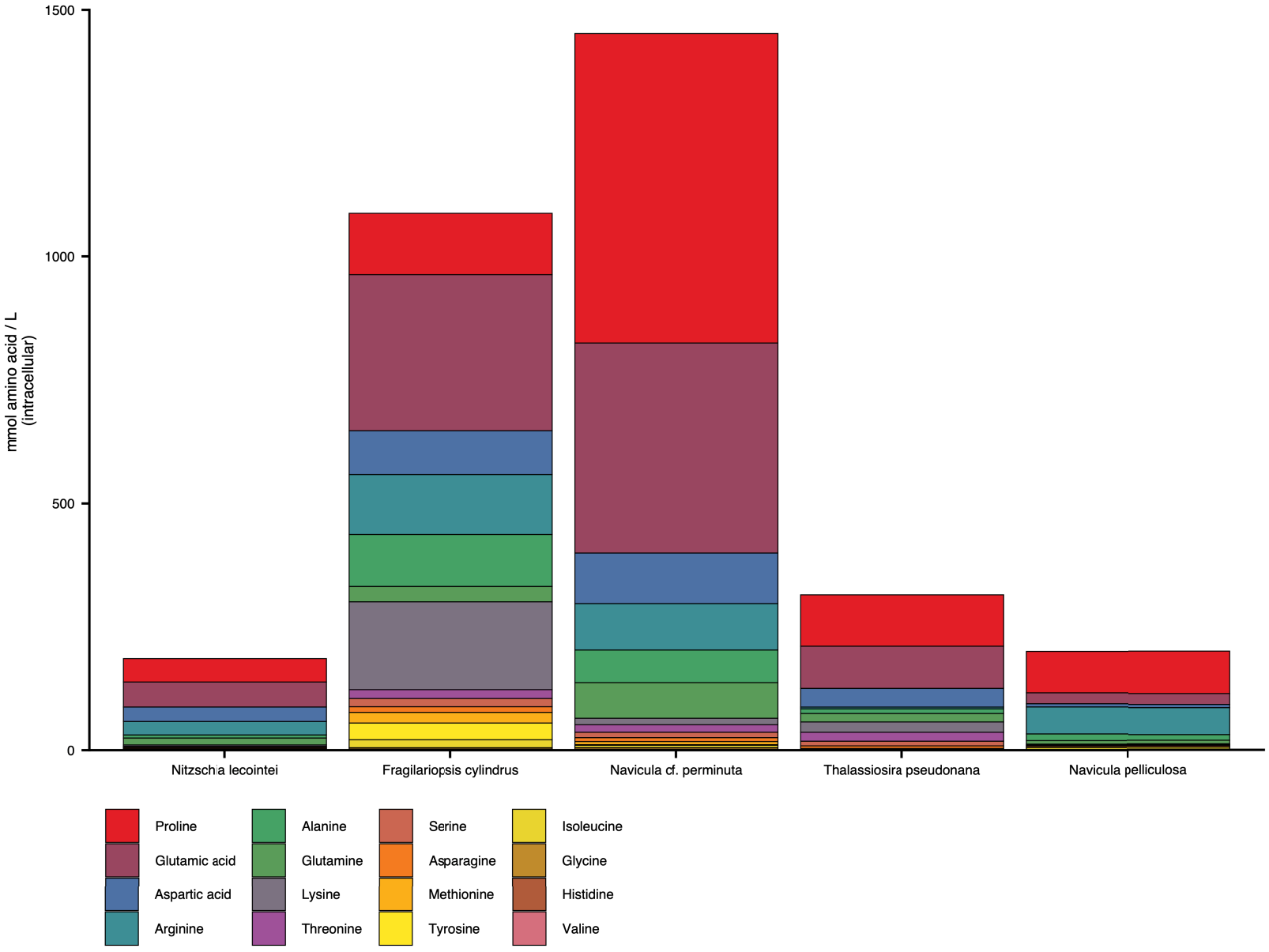
1500
1000
500
0
mmol amino acid / L
(intracellular)
Nitzschia lecointei
Fragilariopsis cylindrus
Navicula cf. perminuta
Thalassiosira pseudonana
Navicula pelliculosa
Proline
Glutamic acid
Aspartic acid
Arginine
Alanine
Glutamine
Lysine
Threonine
Serine
Asparagine
Methionine
Tyrosine
Isoleucine
Glycine
Histidine
Valine